Received: 24 July 2020 | Revised: 17 August 2020 | Accepted: 27 August 2020

DOI: 10.1002/eom2.12054

REVIEW

EcoMat FUNCTIONAL MATERIALS FOR GREEN ENERGY AND ENVIRONMENT WILEY

Recent advances in wearable textile-based triboelectric generator systems for energy harvesting from human motion

Bao Yang | Ying Xiong | Kitming Ma | Shirui Liu | Xiaoming Tao

Research Center for Smart Wearable Technology, Institute of Textiles and Clothing, The Hong Kong Polytechnic University, Hong Kong, China

Correspondence
Xiaoming Tao, Research Center for Smart Wearable Technology, Institute of Textiles and Clothing, The Hong Kong Polytechnic University, Hong Kong, China.
Email: xiao-ming.tao@polyu.edu.hk

Funding information
Hong Kong Polytechnic University, Grant/Award Number: 1-BBA3; Innovation and Technology Commission, Hong Kong, Grant/Award Number: ITP/039/16TP; Research Grants Council, University Grants Committee, Grant/Award Numbers: 525113, 15215214, 15211016, 15200917

Abstract

Large-area, flexible, and light-weight textile-based triboelectric generator (TTEG) technologies are promising power supplier by harvesting energy from human motions, wind, and water current. Numerous TTEG systems have been demonstrated. However, the challenges in their applications include the low electric output power, failure under wearing conditions, and adverse effects on the wearable performance like comfort and durability. What is the influence of system integration on the output performance of the TTEGs? What kinds of textile-structures have the most promising performance? How to make an effective TTEG system? In an attempt to answer these important questions, a critical review is presented on the recent advances of wearable TTEG systems in terms of textile structures, selection of materials, working modes, mechanisms of triboelectrification and charge transfer, energy storage, and their integrations. Furthermore, the major approaches or directions for improving the total conversion efficiency and performance of wearable TTEG systems are systematically summarized.

KEYWORDS

energy harvesting, human motion, textile-based triboelectric nanogenerators, wearable electronics

1 | INTRODUCTION

The rapid advancement of portable electronics greatly enriches the approaches people communicate with each other and with the surrounding environment, which provides more convenience and more accurate information inside human bodies and from the surrounding environment. Up to now, trillions of mobile electronic devices are distributed in every corner of the world, which has integrated the world into an intelligent information network via wire/wireless communication. At the same time, massive energy and batteries are being consumed. However, these batteries have shortcomings of limited use-time thus require frequent charging and heavyweight,[1] which pushes us to develop a green and more user-friendly way to power wearable electronics in future.

Energy presents inside our bodies and in our surrounding environment ubiquitously with different forms, including those in kinetic, elastic, thermal, radiative, and chemical form. The conversion from chemical to

kinetical and thermal energy inside human bodies are not precisely controlled, hence remarkable quantities of energy are dissipating into the surrounding environment.[2] A living human body can be an inexhaustible and cost-free power source, meanwhile it is the application terminal of wearable electronics.

A great number of conversion devices or generators have been investigated to harvest mechanical energy from human motions,[1-10] solar energy and thermal energy in surrounding environments.[11-15] Piezoelectricity, triboelectricity, and electrostatic induction are the most common principles used for transducing biomechanical energy from human motions into electricity. Piezoelectricity mainly generates body-charge (inside matters), which relies on the polarization of charges due to the crystalline structure under deformation. Triboelectricity generators surface charge through frictional contacts between matters. A higher effective surface density can be achieved by triboelectricity than that of piezoelectricity. The electric current in the generator systems is induced by electrostatic induction, which significantly relies on the induction distance and effective charge density. Therefore, the triboelectric generators normally have a higher output power than the piezoelectric generator because of the higher surface charge density and shorter induction-distance in triboelectric generators. More importantly, they can work with a very low level of the applied force, unlike piezoelectric generators whose output is dependent on the deformation under applied forces. Thus the conversion efficiency is higher as a result of lower heat dissipated with inelastic deformation.

Meanwhile, fibrous structures like textile fabrics can effectively accommodate mechanical deformations induced by body movement. If designed appropriately, textile-based triboelectric generators (TTEGs) are wearable, breathable, comfortable, structurally flexible, mechanically robust, low-cost in implementation, and large-scale production. The triboelectric generation has existed in textiles, referred as static charge, even they were made thousands of years ago. It has been regarded as a negative effect and should be reduced. In contrast, the challenge for TTEG is to harvest a sufficient level of mechanical energy from human motion by the integration of triboelectric units in textile architectures unobtrusively.

Up to now, although TTEGs have been extensively reported, their power outputs are still far less than the actual demand of most wearable electronics.[1] Low power output is the bottleneck in the practical application of TTEGs. Several approaches have been developed to improve the energy conversion efficiency by increasing the effective contact area, improving softness, establishing a nanostructured contact interface, using hybrid energy harvesters, or using combinations of multiple approaches.[16] However, by far, there has been a lack of systematic knowledge of TTEGs, which hinders their progress in research and real applications. For example, the mechanical energy available to be harvested from human motions is normally in a discontinuous manner at a lower frequency, often intermittent, and unpredictable. The current TTEGs do not effectively convert mechanical energy into electricity. A large proportion is still in the form of mechanical energy or heat dissipated into the surrounding environment. Numerous approaches have been investigated, among which a promising one is to store the unconverted mechanical energy then releases it gradually and purposefully, so that this energy can be converted into electricity fully.

Herein, a comprehensive, systematic, and critical overview of the working mechanisms, material selections, textile structures, harvesting circuits, features of human motions, and their integrations is necessary for charting the way ahead for TTEG systems with high power output. Furthermore, the challenge and future research directions in the related field are deliberated.

2 | FEATURES OF HUMAN MOTION

Human motion and its features should be known first for harvesting energy from them. The amount of energy used by the body is up to 1.07×10^7 J/d,[17] which is equivalent to the energy of a fully charged battery (3.3 V) with a capacity of approximately 450 000 mAh. The considerable amounts of human energy were released from the body in the main forms of mechanical energy (motion) and thermal energy (heat). During the motion, muscles perform positive mechanical work to generate motion and negative mechanical work to absorb energy and act as brakes to stop the motion.[18] An energy harvesting device should replace part of the muscle activity during the negative work phase so that the device converts energy into electricity with minimal or no interference with natural motions. As shown in Figure 1A, the major body motions during walking are heel strikes and joint motions of the ankle, knee, hip, shoulder, and elbow, which can be considered as potential energy sources.[19] And the related negative work of the muscles as the available power is also illustrated. The max available energy exists on the lower limb motion, like knee (33.5 W), ankle (18.9 W), and hip (7.22 W) joint motion, and heel strikes (1-10 W). However, these actions do not induce a huge change in the contact area between human skin and textiles or between textiles. Arm motion refers to the backward and forward swinging movement of the arms that is composed of two sub-motions: the relative

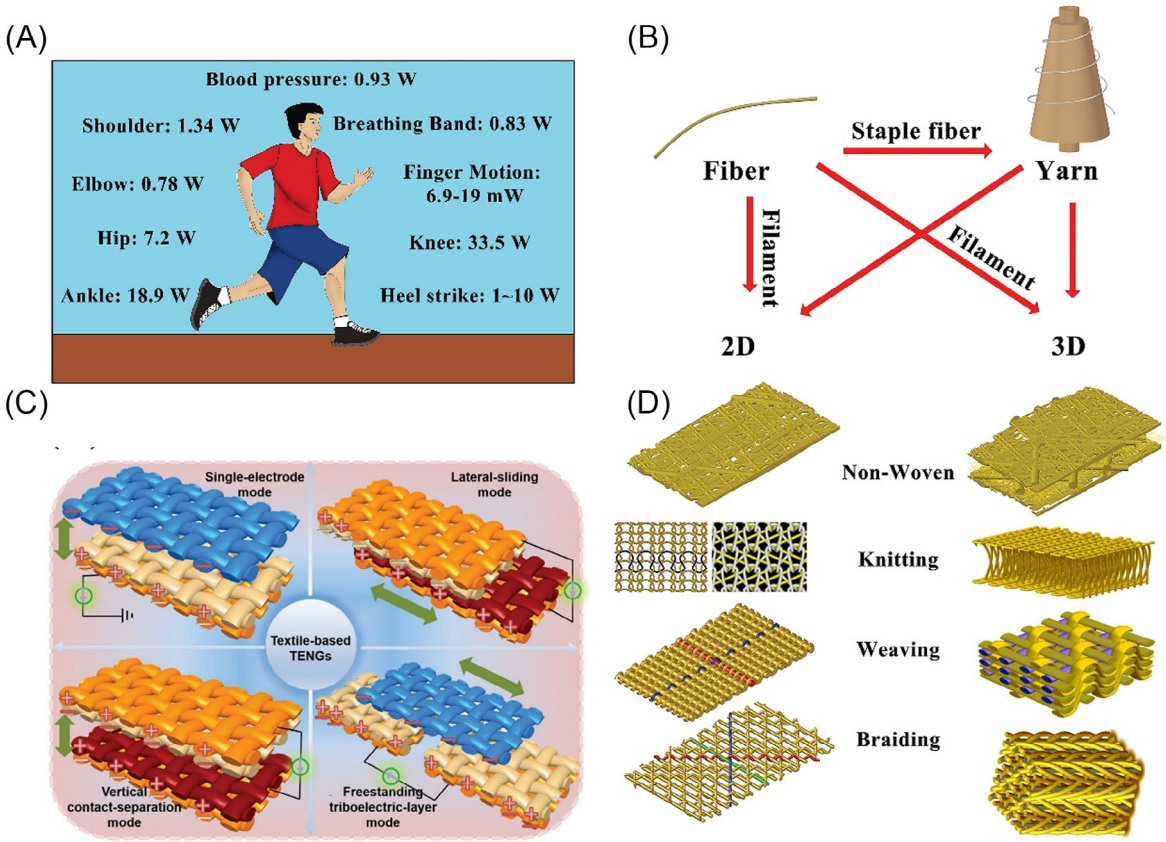

FIGURE 1 A, Available power for everyday bodily activities of human beings, the data were from the Reference 19, assuming an 80-kg person was walking at a frequency of 1 Hz per cycle, and the walking speed of approximately 4 km/h. B, Illustration of textile structures from fiber to 2D/3D textile structures and manufacturing techniques, including nonwoven, knitting (2D weft knitting and warp knitting, reproduced with permission: Copyright 2019, Polymers[41]; 3D structures, reproduced with permission: Copyright 2020, Polymers),[42] weaving (2D structures; 3D structures: reproduced with permission: Copyright 2019, Elsevier),[43] and braiding (2D structures; 3D structures: reproduced with permission: Copyright 2016, Elsevier).[44] C, Schematic of four basic modes of TTEGs, including single-electrode mode (SE), lateral-sliding mode (LS), vertical contact-separation mode (CS), and freestanding triboelectric-layer mode (FT). Reproduced with permission, Copyright 2019, John Wiley and Sons[1]

motion between the forearm and the upper arm (change of angle of the elbow) and the relative motion between the trunk and the upper arm (change of angle at the shoulder).[13] The motion between the trunk and the upper arm can easily make a relatively large change in the contact area between the arm and the upper outer garment. Moreover, the maximum ground reaction force acting on the shoe is approximately equal to 1.2 times the body weight, and most of the heel compression occurs directly after the heel strike.[19,20] And the motion frequency is low like the leg motion with ~1 Hz for walking and 3 to 10 Hz for running. The human angular velocity for a typical joint motion is ~20 rpm. The walking and running speed of healthy young subjects are 0.75 to 1.75 m/s and ~5 m/s,[21-23] respectively. Normally, the arm swing and leg swing are 0.8[24] and 1.3 m/s,[25] respectively. When considering a particular motion as a candidate for energy harvesting, the above features of human motion must be taken into consideration.

3 | WEARABLE TTEGs

Energy from human motion normally is not continuous, low frequency, often intermittent and unpredictable. As a versatile mechanical energy harvesting technology, TTEGs can convert such irregular mechanical energy into electricity via the coupling of triboelectrification and electrostatic induction.[26-29] The TTEG has been demonstrated to harvest mechanical energies of human motions, aiming to be wearable power sources or active self-powered sensors.[30-38] Ever since the first report of the triboelectric nanogenerator (TENG) in 2012 by Wang et al, the areal output power density reaches 500 W/m^2, and the efficiency of TENGs can be up to 85% or higher

TABLE 1 Comparison of textile-based triboelectric generators with four working modes

Modes	TNG structures	Testing structures	Size (cm^2)	Peak voltage (V)	Peak current (μA)	Peak power density (mW/m^2)	Key parameters and influence[a]
SE[45]	Coaxial	Fiber	177	200	100	846	SE: $\sigma\uparrow, x_{max}\uparrow, S\uparrow, f\uparrow$
SE[46]	Coaxial	Knitting	16	150	0.29	85	
SE[47]	—	Knitting	57	190	—	1768	
SE[48]	Coaxial	Woven	2	43	0.51	6	
SE[49]	Coaxial	Woven	18	354	15.6	8	
SE[50]	Coaxial	Woven	—	40	4	127	
SE[34]	Core-shell	Woven	36	75	1.2	60	
SE[51]	Fabric-based	Film	25	13	1.75	3	
SE[52]	Fabric-based	Film	4	18	1.5	130	
SE[53]	Fabric-based	Film	9	47.1	7	144	
SE[54]	Fabric-based	Film	8	262	8.73	2859	
SE[55]	Fabric-based	Film	65	340	78	13 200	
SE[56]	Film-based	Film	6.25	250	—	17	
SE[57]	Film-based	Film	29.5	1000	—	500	
SE[58]	Film-based	Film	37.5	700	75	5000	
SE[59]	Film-based	Film	2.25	270	11	25 000	
LS[60]	Fabric-based	Film	100	22	0.37	0.004	LS: $\sigma\uparrow, S\uparrow, f\uparrow$
LS[61]	Fabric-based	Film	13.5	15	0.13	1.8	
CS[62]	Coaxial	Fiber	—	80	0.4	31	CS: $\sigma\uparrow, x_{max}\uparrow, S\uparrow, f\uparrow, d_0\downarrow$
CS[63]	Core-shell	Fiber	—	0.66	0.02	0	
CS[64]	Core-shell	Fiber	—	3.22	—	1	
CS[65]	Core-shell	Fiber	35	140	—	2	
CS[66]	Core-shell	Knitting	—	9.1	0.1	1	
CS[67]	Fiber-based	Knitting	48	206	28.7	30.4	
CS[68]	Core-shell	Woven	0.6	0.2	0.01	0.04	
CS[69]	Fabric-based	Woven	25	50	4	128	
CS[70]	Fabric-based	Woven	25	50	4	400	
CS[71]	Fabric-based	Film	1	234	11	1.7	
CS[72]	Fabric-based	Film	20	150	2.5	4	
CS[73]	Fabric-based	Film	9	575	12.1	2800	
CS[74]	Fabric-based	Film	5	253	—	7600	

TABLE 1 (Continued)

Modes	TNG structures	Testing structures	Size (cm^2)	Peak voltage (V)	Peak current (μA)	Peak power density (mW/m^2)	Key parameters and influence[a]
CS[75]	Fabric-based	Film	20	2209	1210	56 900	
CS[76]	Fabric-based	Film	49	259	78	336 000	
CS[77]	Film-based	Film	16	153	23	0.03	
CS[78]	Film-based	Film	45	428	1395	31	
CS[79]	Film-based	Film	243	220	40	58	
CS[80]	Film-based	Film	4	161	6	226	
CS[81]	Film-based	Film	29.6	700	—	352	
CS[82]	Film-based	Film	36	840	55	2036	
CS[83]	Film-based	Film	14.4	215	0.66	98 000	
FT[84]	Fabric-based	Knitting	8	19	1.8	94.5	FT: $\sigma\uparrow, x_{max}\uparrow, S\uparrow, f\uparrow, d_0\downarrow, g$
FT[85]	Fabric-based	Film	25	255.5	1.15	832	

Note: The effective surface charge density on the dielectric layer (σ), the maximum gap distance between the dielectric layer and the electrode (x_{max}), the effective gap distance between two fixed electrodes (g), the effective thickness of dielectric layers (d_0), the contact surface (S), contact-separation frequency (f), ↑ means more charge will be transferred at the higher value of the parameter and ↓ is reverse.
[a]The influence on the average transferred charges ($\bar{Q}$) at the short-circuit condition and the mean output power ($\bar{P}$).

based on a and well-controlled and extremely small mechanical input.[39,40] However, such small mechanical input rarely exists in our daily life. Efficient conversion-structures are highly desirable for TEGs by reducing internal consumption.

The working modes, the structural characteristics, testing structures, the main outputs, and the key parameters and their reference on the transferred charge and the output power of wearable TTEGs are summarized and compared in Table 1. According to the structures of functional components, TTEGs can be divided into three categories: fiber-based (coaxial or core-shell), fabric-based, and film-based TTEGs. Coaxial-fiber means that the dielectric polymer wrap around the core fiber electrodes, normally in single-electrode mode TTEGs. Core-shell-fiber contains an inner fiber-electrode and an outer encapsulated sheath as the dielectric layer. The fabric-based TTEG is produced by narrow thin films or cloth stripes. The film-based TTEG is fabricated on film substrates and then laminated on textiles. The demonstrated output power of TTEGs with textile-structures, including fiber (~846 mW/m^2), knitting (28.7 mW/m^2), and woven (400 mW/m^2), are much lower than those measured in film-shapes with the fabrication of fabric-based (336 000 mW/m^2) or film-based (98 000 mW/m^2). Moreover, a series of interacting factors will influence the output performance of TTEGs. Hence, a systematic analysis of these factors is necessary.

3.1 | Textile-structures

The textile structures can be of one or multi-dimensions, made by different manufacturing techniques, as shown in Figure 1B. Fiber is the fundamental and visible unit of textiles. By assembling/interlocking fibers with twisting, twining, or texturing, along the axial direction, one-dimensional (1D) yarns can be formed. The yarns or filament fibers can further be integrated into two-dimensional (2D) or three-dimensional (3D) textiles using weaving, knitting, braiding, and nonwoven methods. Woven, knitted, nonwoven, and braided fabrics are common fabrics made with mass production processes. In woven fabrics, two groups of yarns (warp and weft) are interlaced orthogonally.[86] According to the interlacing patterns, woven fabrics have various structures of plain, twill, and satin. The woven fabrics exhibit very strong anisotropic mechanical properties: they are relatively inextensible in the warp and weft directions but opposite in the bias direction. The large in-plane shear of woven fabrics contributes to the 3D deformability.

The knitted fabric has meandering and suspended loops, which can be easily stretched in all the directions and possess a much lower Young's modulus than other types of textiles. Knitted fabrics include weft-knitted and warp-knitted fabrics. In terms of fabrication, weft knitting is the easiest as a single yarn can be used to knit fabrics, while hundreds of yarns through beaming are necessary for warp knitting and weaving. Nonwoven fabrics consist of individual fibers, in which staple fibers or filaments are oriented or randomly arranged to form a network structure, then reinforced by mechanical, thermal adhesive, or chemical methods.[87] With the advantages of short technological processes, fast production rate, high output, low cost, nonwoven fabrics have wide applications in health care, industry, and farming, while most of them have poor strength, abrasive resistance, and durability. Therefore, nonwoven fabrics are rarely utilized in TTEGs. Braided fabrics are formed by interweaving three or more strips in a diagonally overlapping pattern. Three dimensional braided fabrics are made by inter-plaiting three orthogonal sets of yarns.[88] Braided fabrics have high strength and stiffness, making them suitable for industrial applications but less utilized in clothing.

If fabrics are used in TTEGs, considerations must be given to its mechanical and surface properties. The linear density of fibers and yarns, mechanical properties of yarns, the structures of fabrics, and the density of fabrics affect the contact surface and mechanical properties of fabrics.[89] Fabric structures may affect the selection of the working mode of TTEGs, which will be discussed in the following section. Woven fabric has the most stable structure in terms of shape-preserving, dimensional stability, and strength, simple structure, relatively smooth surface, large top-surface area, and low thickness, which is suitable for TTEGs, showing a relatively high output power. Knitting-fabric is widely utilized in SE mode TTEGs due to its good extensibility, low modulus, and high porosity, especially for human-interactive applications where large deformation is required. But they also are prone to pilling, snagging, and easily deformed, which limits their applications in wearable LS or FT mode TTEGs. Nonwoven and braided textiles are rarely utilized in TTEGs yet due to their above shortcoming in processes and applications.

3.2 | Mechanism and working modes

Contact electrification (also called triboelectrification) and induction charge transfer are the two major phenomena involved in TTEG systems. The concept of triboelectrification by electron transfer has been well accepted in explaining metal-metal, metal-semiconductor, and metal-insulator contact system.[90-93] Ion transfer was also proposed to explain the contact electrification in involving polymer contact systems,[94-97] in which ions containing functional groups were believed to have a great contribution to contact electrification. Recently, inspired by the atomic or molecular orbits model, the electron cloud-potential well model is proposed to illuminate the contact electrification mechanism for all types of two interactive-materials systems.[98] A curvature-dependent charge transfer model was established to explain the contact electrification between two identical materials.[99] More important findings are obtained, including electron thermionic emission dominant deterring factor at high temperature, an upper limit of temperature that triboelectric generator can work, and a potential barrier at the surface that prevents the generated charges flowing back to the solid where they are escaping from the surface during the contact-separation process.[98,100] These results can partly explain that the surface charges generated in contact electrification are readily retained by the material. In contrast, the second phenomenon of induction charge transfer is relatively well understood. Theoretical equations of the voltage and power output from the four modes of TTEG summarized below are testimony of the progress in this regard.

As shown in Figure 1C, TTEGs can be categorized into four different operational modes, following Wang's proposal, that is, single-electrode (SE) mode, lateral-sliding (LS) mode, vertical contact-separation (CS) mode, and freestanding triboelectric-layer (FT) mode according to the circuit connection methods and the separation direction of contact surfaces.[1] SE-mode TTEG is simple that only one electrode is needed to connect with the measurement device, but its output normally is low and has weak stability. LS-mode TTEG is compact in the vertical direction and separates in the contact-surface direction so that parallel-contact-surface is desirable. Its output is relatively high and continuous, but its friction surfaces are easily damaged. CS-mode TTEG separates in the vertical direction, which also has simple devices and high output. FT-mode TTEG has two fixed electrodes, high energy conversion efficiency. But their structures are too complex to integrate. From electrodynamics, the governing equation, that is the *V-Q-x* relationship, for these four modes triboelectric generators can be given as the following equation.[101]

$$V = -\frac{Q}{C} + V_{OC}, \tag{1}$$

where V is the voltage between the two electrodes. V_{OC} is the voltage between the two electrodes at the

open-circuit condition, C is the total capacitance, and Q is the amount of transferred charged between the two electrodes, driven by the induced potential. Although the working mechanism of four working modes is same, that is the coupling effect of triboelectrification and electrostatic induction, each mode has its specific characteristics because C and V_{OC} rely on the working mode and structures of TENGs. And then, the main outputs of the average transferred charges ($\bar{Q}$) at the short-circuit condition and the instantaneous output power (P) for four working modes are given below, respectively.

1. SE-mode (when x/l and g/l are close to 0)[101]:

$$\bar{Q} = \frac{f\sigma w x_{\max}}{\pi}\ln(l), \tag{2}$$

$$P = \left[\frac{\sigma g x}{\pi\varepsilon_0 l}\ln(l) - \frac{g}{R\varepsilon_0 w l}e^{-\frac{gt}{R\varepsilon_0 w l}}\int_0^t \frac{\sigma g x}{\pi\varepsilon_0 l}\ln(l)e^{\frac{g\tau}{R\varepsilon_0 w l}}d\tau\right]^2 R, \tag{3}$$

where σ is the effective tribo-charge density, g is gap distance between electrodes, f is the frequency of contact-separation, and w and l are width and length of dielectric, x and $x_{\max}$ are the separation distance and its maximum, ε_0 is the permittivity of air, and R is the external resistance.

2. LS-mode (when the electrode is moving at a constant speed v)[102]:

$$\bar{Q} = 2f\sigma w x_{\max}, \tag{4}$$

$$P = \left\{\sigma w v\frac{d_0}{Rw\varepsilon_0 v - d_0}\left[\frac{l}{l-vt}e^{\frac{d_0}{Rw\varepsilon_0 v}\ln\left(\frac{l}{l-vt}\right)} - 1\right]\right\}^2 R, \quad \text{for } Rw\varepsilon_0 v \neq d_0 \text{ and } t < l/v, \tag{5}$$

$$P = \left[\sigma w v\ln\left(\frac{l-vt}{l}\right)\right]^2 R, \text{ for } Rw\varepsilon_0 v = d_0 \text{ and } t < \frac{l}{v}, \tag{6}$$

where d_0 is the effective thickness of dielectrics.

3. CS mode[103-106]:

$$\bar{Q} = 2f\frac{S\sigma x_{\max}}{d_0 + x_{\max}}. \tag{7}$$

$$P = \left[\frac{\sigma x}{R\varepsilon_0} - \frac{d_0 + x}{RS\varepsilon_0}e^{-\int_0^t \frac{d_0+x}{RS\varepsilon_0}d\tau}\int_0^t \frac{\sigma x}{R\varepsilon_0}e^{-\int_0^\tau \frac{d_0+x}{RS\varepsilon_0}dz}d\tau\right]^2 R. \tag{8}$$

4. FT mode (for a single frequency harmonic vibration $x = A_0 + A_0\sin(\omega t)$)[107]:

$$\bar{Q} = 4f\frac{S\sigma x_{\max}}{d_0 + g}, \tag{9}$$

$$P = \left[\frac{2\sigma A_0}{\varepsilon_0}\frac{\omega\varepsilon_0 S(d_0+g)}{(d_0+g)^2 + \omega^2\varepsilon_0^2 S^2 C^2}\left(\omega R\frac{\varepsilon_0 S}{d_0+g}sin(\omega t) + \cos(\omega t)\right)\right]^2 R, \tag{10}$$

where S is the area size of the dielectrics, ω is the vibration angular speed, and A_0 is the varibation anplitude.

The time-averaged output power ($\bar{P}$) can be given below

$$\bar{P} = f\int_0^{1/f} P dt. \tag{11}$$

From the above mathematical models, higher surface charge density, larger effective contact area, larger maximum separation distance, and higher contact-separation frequency are benefitted to have a higher output, while the dielectric layer with a lower effective thickness is better. In these theoretical analyses, several basic assumptions also have been made, including parallel-plate

structures, equivalent capacitance with neglected edge effects, stable and uniform surface charge density, the uniform gap in contact and separation, and uniform thickness of dielectric layers. However, these assumptions may become not true when TENGs were fabricated with textile structures, which may lead to much lower output power. TTEGs can be easily designed with single fibers, yarns, fabrics, or laminated architectures, in woven or embroidered form, or by lamination on the surface of textile fabrics.[108] The TTEGs fabricated by using fabric and laminated fabric architectures exhibit much higher output voltage than those fabricated by using coaxial or core-shell fiber methods. Such results indicate that though TTEGs can be integrated with textiles, there are still some fundamental issues that should be considered carefully in structural designs, including:

1. Effective surface charge density relies on the local distribution of surface charge density and the real contact area. The textiles normally have a large porosity that reduces with increasing pressure. It influences the internal electric field and reduces the amount of charge transferred to half of the sold materials, as an experimental observation. From the theoretical analysis of TTEGs with parallel-plate-structures, the effective surface charge density possesses a quadratic (the highest order) effect on the output power.
2. The edge effect means that the magnitude of the electric field at the zone near edges is much smaller than that in the middle zone. For the same surface charge density, more zones with edge effect cause a much lower magnitude of electric field and electric potential difference. The surfaces of textiles have multiple level structures from fibers to fabrics. Most of the contact zones on the top surface are isolated, which induces a high edge effect. Thus, less charge was transferred due to electrostatic induction.[109]
3. Effective contact-separation frequency significantly affects the mean output power. Although TTEGs can work on low-frequency mechanical inputs and even their outputs have high peak values, their average output over time is still low. Each contact-separation will result in two times charge-flows due to electrostatic induction. More charge flows, higher output normally is achieved. Therefore, TTEGs work on a high frequency, which can be an effective approach to significantly enhance the outputs. Yet, an effective way that can translate the low frequency and irregular mechanical input from human motion into a high-frequency contact-separation of the triboelectric units in smart textiles is lacked.
4. Due to the limitation of air-breakdown and filed emissions, the effective surface charge density has an upper limit in the ambient environment. Therefore, achieving a larger effective contact area can be an effective approach to add the total surface charge for higher output. And the weaving textiles with a relatively flat surface were popular in CS and LS-mode TTEGs. However, such CS or LS-mode TTEGs usually laminate on a fabric substrate. To maintain a flat surface, TTEGs become relatively rigid, which reduces the conformability. Therefore, more reasonable textile-structures are necessary for TTEGS.
5. The effective separation distance is also necessary. From the theoretical analysis of parallel-plate TTEGs, higher separation distance will lead to more charge transferred from one electrode to other electrodes. Especially, the fiber-shaped CS or FT-mode TTEGs have a very small gap due to the small diameter of fibers. How to make an effective separation is crucial for high output power.

3.3 | Selection of materials

All types of materials can be candidates for fabricating TTEGs because contact electrification can exist between any contact surfaces made of different materials and even the same materials. However, the residual charge on the contact surfaces significantly affects the final output performance of the TTEGs. Accordingly, the triboelectric series of materials, created based on the measurement of the residual surface charges, is the main principle of material selection for TTEGs previously. A series of triboelectric series have been developed by summarizing the results of the previous studies, adding more materials or/and adding more testing conditions with more accurate control and the related description.[2,27,110-114] But conflicting orders among different triboelectric series exists due to the different measuring methods. Recently, a universal method has been investigated to quantify the triboelectric series for a wide range of polymers and inorganic non-metallic materials by measuring the tested materials with liquid metal under well-defined conditions.[113,114] However, this triboelectric series highly rely on the surface viscosity between the object material and liquid metal, which also cannot be extended to most of the applications. As well as many materials will not be utilized to textile structures due to their basic material characteristic like rigid and crispy as well as high-cost in processing.

If the structure changes from simple plates to textiles, porosity, structures in terms of fiber, yarn or fabric, locally curved surface, flexibility, deformation, and moisture regain should be considered carefully in the selection of materials. If fabrics normally are porous and

TABLE 2 Measured charge densities of plain knitted fabrics and key materials properties materials

Fiber materials	Yarn speciation	Effective charge density nC/cm^2 (CV)	Nominal charge density nC/cm^2 (CV)	Reported charge density nC/cm^2	Elastic modulus (GPa)	Breaking strain (%)	Moisture regain (%)
Polytetrafluoroethylene (PTFE)	210D	−2.750 (23.00%)	−1.550 (14.00%)	−0.020, −0.700, −3.000	0.564[143]	40.0[143]	0.00[144]
Polyethylene (PE)	210D/48f	−1.260 (11.20%)	−0.900 (7.30%)	−0.500	0. 200[145]	12.9[146]	0.01[147]
Polyimide (PI)	210D/48f	−0.473 (2.30%)	−0.370 (4.50%)	−0.001	0.107[148]	15.5[148]	0.07[148]
Polypropylene (PP)	20Ne	−0.312 (12.50%)	−0.230 (3.46%)	−0.001	4.910[149]	17.0[149]	0.00[149]
Polyparaphenylene terephthalamide (Kevlar)	210D/108f	−0.112 (3.46%)	−0.070 (2.45%)	Nil	78.430[149]	2.4[144]	3.50[144]
Polyethylene terephthalate (PET)	210D/108f	−0.109 (4.50%)	−0.067 (3.56%)	−0.001	10.780[149]	14.5[149]	0.40[149]
Polyacrylonitrile (PAN)	32Ne	−0.065 (2.45%)	−0.045 (4.51%)	0.00039	2.250[150]	4.0[151]	0.85[150]
Cotton	32Ne	0.011 (2.30%)	0.005 (2.45%)	0.0012-0.0015	3.300[152]	6.5[149]	8.50[151]
Ramie	32Ne	0.029 (1.39%)	0.010 (2.34%)	0.0012-0.0015	24.500[149]	3.6[149]	12.00[149]
Beta-poly-D-glucosamine (chitosan)	32Ne	0.034 (4.32%)	0.016 (4.55%)	Nil	7.677[153]	7.61[153]	16.41[153]
Fiberglass	180D/108f	0.105 (4.56%)	0.055 (3.52%)	Nil	72.000[154]	3.0[154]	0.00[154]
Wool	32Ne	0.142 (3.43%)	0.068 (1.34%)	0.005-0.009	2.900[149]	25.0[155]	13.00[155]
Cuprammonuium (Cupro)	75D/48f	0.159 (2.38%)	0.079 (3.45%)	Nil	Nil	8.8[156]	12.500[157]
Lyocell (cellulose fiber)	75D/48f	0.163 (1.33%)	0.081 (2.41%)	Nil	8.000[158]	14.0[158]	11.00[159]
Polycaprolactam (Nylon 6)	210D/108f	0.283 (2.40%)	0.150 (4.65%)	0.005-0.009	2.950[160]	30.0[160]	4.50[144]
Silk	32Ne	0.342 (4.56%)	0.180 (3.44%)	0.005-0.009	6.500[161]	25.0[162]	11.00[162]
Polyurethane	40D	0.385 (9.84%)	0.200 (4.45%)	0.005-0.009	0.690[163]	375.0[164]	0.20[163]
Poly[imino (1,6-dioxohexamethylene) iminohexamethylene] (Nylon 66)	210D/108f	0.422 (5.55%)	0.230 (5.66%)	0.005-0.009	3.720[165]	3.0[165]	4.50[166]
Poly(3-hydroxybutyrate-co-3-hydroxyvalerate) (PHBV)	75D/48f	0.453 (3.56%)	0.240 (6.74%)	Nil	Nil	2.8[156]	0.250-0.710[167]
Polylactide/poly (3-hydroxybutyrate-co-3-hydroxyvalerate) (PLA/PHBV)	75D/48f	0.643 (4.24%)	0.320 (6.73%)	Nil	2.01[156]	26.8[156]	0.40[156]
Polylactide (PLA)	75D/48f	0.872 (3.56%)	0.480 (3.57%)	Nil	3.50[168]	11.3[168]	0.45[169]

Note: The first five columns are from Reference 111. "D" stands for denier, linear density in g/9 km; *f* is the number of fibers; and Ne is the English yarn count, the length of 770 m in 0.45 kg.

deformable, the effective contact-surface area will highly increase if the applied pressure increases before reaching the fabric densification. A textile-related triboelectric series including 21 types of commercial and new fibers have been investigated, as shown in Table 2,[111] which is constructed based on a sliding-mode triboelectrification system. It is found that the effective charge density of fabrics can be reliably measured when the triboelectrification process reaches its saturation under the fabric densification pressure, showing that there is no significant difference between the triboelectric series measured on the planner films and textiles under a fabric densification pressure. But there is a huge difference between the charge density using nominal and effective contact areas. Therefore, the mechanical properties of the textile become significantly important due to the structural hierarchy of textiles.

Moreover, more interact factors such as polarity, flexibility, softness, wearability, and humidity play significant roles on the output of wearable TTEGs. Polarity can be selected from the triboelectric series, showing the upper limit of the local surface charge density. Elastic modulus and breaking strain affect the contact area and wearability. Moisture regain mainly affects the humidity on the surface. These important properties of materials also have been added in Table 2 for a comprehensive consideration in the selection of materials. In terms of textile structures, woven textiles are suggested to be utilized in parallel contact-surfaces or symmetrical contact-surfaces due to their simple, relatively smooth with a large top surface area, stable structure, and good durability. And knitted textiles are suggested to be utilized in asymmetric and easily changeable contact-surfaces due to its merits in good elasticity and ease of deformation. Yet, due to the complexity in the practical applications with different priorities in performances, a standard method is still lack to guideline the selection of materials.

Another important selection of materials is for the electrode made of conductive materials. The electrodes in textiles can be different shapes like the core of the fiber, shell, planar or other shapes. Ideally, the introduction of electrodes integrated into textiles should be safe and have a neglected negative effect on the original performance of textiles. The commonly used conductive materials for textiles can be divided into several types in terms of element compositions and conductive mechanisms, including metals and metallic derivatives, conductive polymers, and conductive liquid. Metal possesses high electrical conductivity, universal existence, strong mechanical stability, and convenient recyclability. However, due to rigid nature, intrinsic brittle, heavyweight, and easy to be oxidized, it is difficult to achieve large scale applications in wearable textiles. Therefore, low dimensional nanostructures metallic derivatives, such as nanoflakes, nanosheets, nanoparticles, nanowires, and nanoclusters, are widely applied to be one kind of significant fillers.[115-120] Through commercial physical depositing, electrodeless plating, or screen-printing methods, metallic nanomaterials are easily adhered to or incorporated in textile systems though these methods have a relatively high cost and low solid content.[121,122] Another kind of fillers is carbonaceous filler like carbon black, carbon particle, carbon fiber, carbon nanotubes, carbon aerogel, graphite, graphene, graphene oxide, and reduced graphene oxide.[123-125] Liquid electrolyte[126,127] and liquid metal[49,128-132] are the two main representatives of liquid electrodes, which are flexible and stretchable conductive materials. But they are mostly toxicity, heavy, ease of leakage, and expensive. Each kind of electrode made of a single mechanism/material has its strength and weakness, which should be chosen carefully according to the practical applications. Meanwhile, hybrid conductive fillers have been attracted many research efforts to make full use of their merits and compensate for the shortcoming of different fillers,[133-142] showing a high potential application in flexible and wearable textile-based electronics. The fabrication methods of smart textiles and the related conductive materials have been summarized recently by Dong et al,[1] which will not be discussed in this review.

TTEGs are mainly for wearable purposes, so they are desirable to have other capacities of washability, breathability, biocompatibility, robustness, and comfortability like the common textiles. Dong et al[1] recently summarized the stretchability/durability and washability of fabric-based TENGs, showing that TTEGs with different modes, including SE, CS, LS, and FT mode, can be washable. A 2D SE-mode TTEG, made of stainless steel wire as electrodes and silicone rubber and skin as the triboelectric materials, showed the largest times of washability (up to 120 times).[34] The durability of a washable SE-mode TTEGs, made of Ag-coated fibers as electrodes and Ag and PAN as triboelectric materials, can be up to 100 000 times.[47] The stretchability of TTEGs can be high over 100%,[31,46,49] but such TTNGs normally have a relatively low output power due to high porosity and less effective contact area. Moreover, the temperature and humidity in the human microenvironment, involved with the permeability of air, moisture, and water, play a significant role on comfortability and breathability as well as the output power of TTEGs. Because the properties, including good flexibility, stretchability, washability, breathability, biocompatibility, robustness, comfortability, and high output power, have adverse interaction and their specific requirements in structures and materials, and thus, these good performances are difficult

to be achieved in a wearable TTEG simultaneously. Therefore, a balance among these capacities should be considered carefully for real applications.

3.4 | Energy storage and system integration

As shown in Figure 2A, energy harvesting, energy storage, and power management are three key parts for harvesting energy from human motion to a green and wearable power supply. At the infant stage of TTEG systems, achievements of the capability of energy harvesting are the main target. However, with the rapid development and continuous research, more requirements such as higher output, higher efficiency, stable, soft, comfort, and less influence on human activities are needed to be realized. The harvesting energy can be directly used or stored as an energy reserve for powering electronics. The most conventional devices for energy storage are supercapacitors and batteries. Supercapacitors show the merits of high-power density, fast charge-discharge rate, and long cyclic stability, while batteries have advantages of high energy density, high working voltage, and low self-discharge properties. They all have limited lifetime and capacity, and frequent recharging or replacement will lead to great inconvenience. To address this problem, system integration of energy harvester, power management, and energy storage devices into textiles could be an alternative approach, so that the environmental energy can be simultaneously harvested and stored for sustainable power supply.

With the rapid development of commercial capacitors or supercapacitors, they become smaller, higher power density, and easy to integrate into textiles. As shown in Figure 2B-D, it is convenient to harvest energy and store it into commercial capacitors or supercapacitors. However, these storage devices are rigid, which affects the appearance and comfort of the textiles. Thence, soft wearable energy storage devices have been developed, which be fabricated in thin-film or fiber/textile structures.[170-172] The fiber/textile-based supercapacitors can be further classified into 1D fiber/yarn structure and 2D fabric architecture. As shown in Figure 2E, the all-textile supercapacitor is build up by the stacking layer of textile materials, including carbon cloths as current collectors, electro-spun polyacrylonitrile nanofibers as separators, and PEDOT nanofibers as both positive and negative active materials.[170] Fiber-shaped supercapacitors (FSCs) also have been widely studied owing to their high flexibility, tailorability, and knittability. An illustrated solid-state FSC (Figure 2F) is fabricated into symmetric structures by assembling two Tin/Ti electrodes, while the KOH/PVA gel is simultaneously used as electrolyte and separator. Such FSCs demonstrate excellent tailorability, superior electrochemical performance (0.36 mF/cm), cycling stability (87.5% capacitance retention after bending 2000 times), and excellent stability (up to no degradation in 60 days).[171] The volumetric energy density and power density of an all-solid-state supercapacitor yarn, fabricated by highly scalable electroless deposition of Ni and electrochemical deposition of graphene on commercial cotton yarns, are up to 6.1 mWh/cm^3 and 1400 mW/cm^3, respectively.[172] Such a supercapacitor yarn is lightweight, highly flexible, strong durable in the life cycle and bending fatigue tests, and ease of integration into textiles (Figure 2F,G).

Aiming to develop comfort and wearable power textiles, Wang et al first reported a fiber-based self-charging power system, which consists of a TTEG and fiber-based supercapacitor.[173] Thereafter, more integration of flexible, wearable TTEG and supercapacitors have also been demonstrated.[174] As shown in Figure 2H, a stretchable and washable all-yarn-based system that integrated knitting a TTEG fabric and solid-state yarn supercapacitors is presented to simultaneously harvest and store human motion energy for powering wearable electronics like a watch.[46] Pu et al also developed a solid-state yarn supercapacitor with reduced graphene oxide as active materials (Figure 2I). Such a yarn supercapacitor exhibited high capacitance (13 mF/cm) and stable cycling stability (96% for 10 000 cycles). A power textile is achieved by weaving the yarn supercapacitors together with a TTEG into a single cloth. Similarly, more yarn supercapacitors together with a TTEG are integrated into a single cloth/ textile, as shown in Figure 2J,K. The above demonstrations have shown the integration of TTEGs and supercapacitors. However, the rectifying circuit is typically separate. More impact packages also have been developed.[175-178] As shown in Figure 2L, an impact package structure-based power system that integrates a SE mode TENG with an MXene-based-micro-supercapacitor into a monolithic device. Such a device can be worn on the forearm and charged by human motion.[175] Normally, a higher voltage across the storage can be obtained at a higher working frequency.

The above methods that directly connect the generators with the supercapacitor/batteries may lead to low energy-storage efficiency due to the mismatch of impedance. To address this problem, power management circuits can be utilized to maximize the efficiency of practical applications. The power-supplying system can provide a continuous direct-current power for driving wearable electronics via a power management circuit that includes a transformer, a rectifier, a voltage regulator, and capacitors/batteries. However, the transformer only

has a satisfied performance at a matched frequency.[179] And then, the enhanced design of a two-stage power management circuit has been developed by Niu et al, which is universally applicable to all types of TENGs with pulsed outputs.[81] With such a power management system, the power system can achieve 60% AC-to-DC efficiency and provide a continuous DC electricity of ~1 mW for continuously driving wearable electronics. Another universal power management strategy has developed for TENGs with higher efficiency (up to 80%) by maximizing energy transfer, DC buck conversion, and self-management mechanism.[180] Different from the

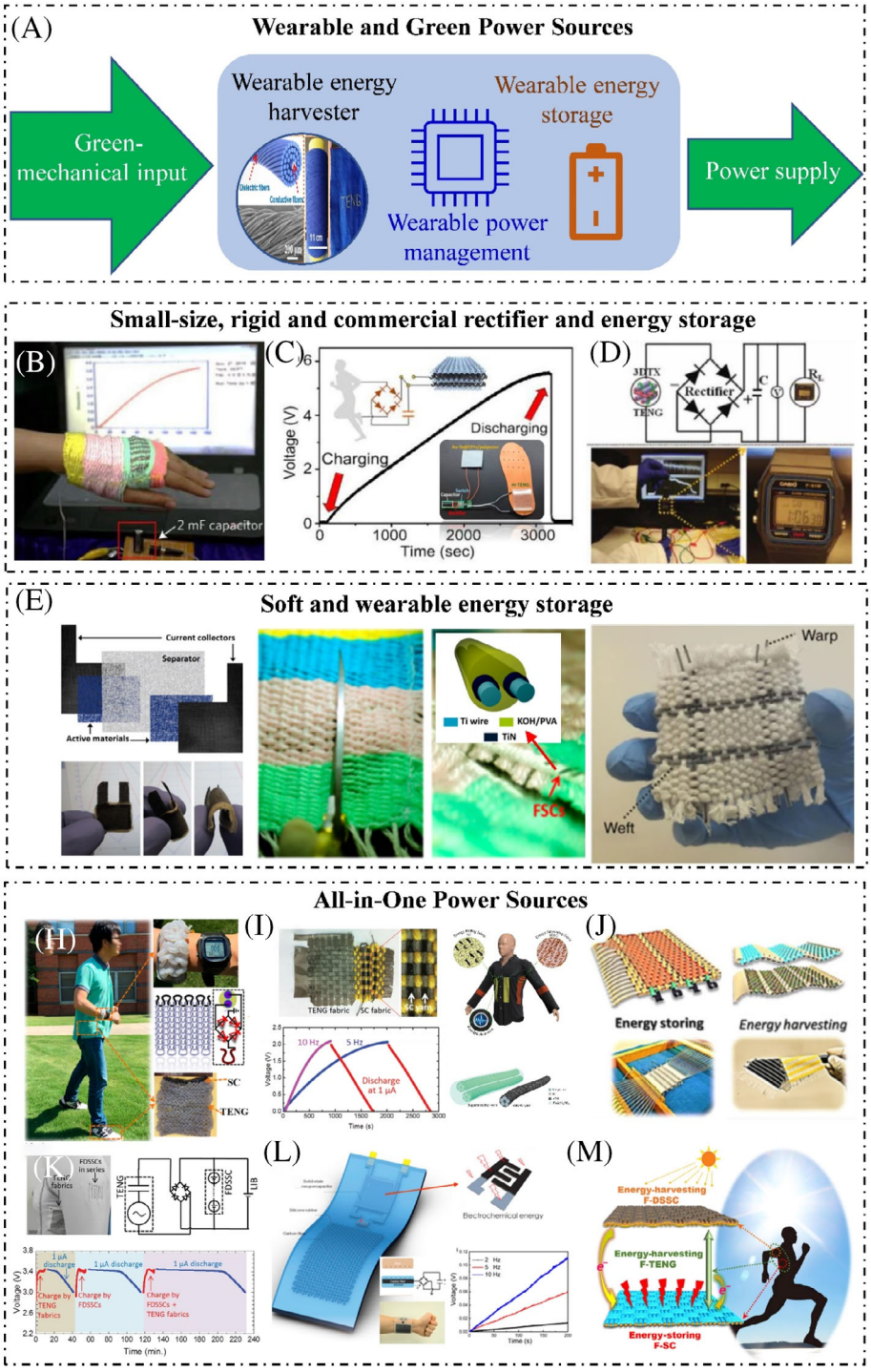

FIGURE 2 Legend on next page.

above inductor-based management circuits, switch-based circuits also have developed for power management.[181-183] The circuit is based on an array of self-connection-switching capacitors. The capacitors are first serial-connected in the charging operation and then connected in parallel for power output. Compared with the direct charging cycle, the designed cycle can enhance the charging rate and improve the energy-storage efficiency (up to 50%). Although using a switch is effective for managing and improving the output performance, its elaborate design will make the system more complicated and expensive. Therefore, future efforts are still needed to improve the efficiency of the management circuit and also reduce their size.

Moreover, to enhance the energy harvesting capability, TTEGs and other energy-harvesting technologies can be combined to form a hybrid energy-harvesting device, so that various types of environmental energy and energy from human motions can be simultaneously scavenged. An all fiber-based hybrid power system has been developed by Wen et al, which converts outdoor sunshine and random body-motion energy into electricity stored as chemical energy in supercapacitors.[184] Because each component of the power system is an all-fiber-shaped structure, the system can be woven into individual fabrics to fabricate smart textiles for powering electronics, as shown in Figure 2M. Similar methods also have been utilized to simultaneously harvest energy from solar light and human motion, where a textile-based grating-structured TENG, fiber-shaped dye-sensitized solar cells, and a lithium battery are employed.[33] Piezoelectricity and triboelectricity are commonly combined in hybrid generators due to lightweight and impact designs, which have been reviewed systematically.[1,3,4,9,10] Electromagnetic generators and thermoelectric or pyroelectric generators also have been developed to combine with TTEGs for harvesting energy from human activities.[185-187] But such combinations have obvious shortcomings of heavy, rigid, or low efficiency at the current state. Overall, hybrid energy harvesters and supercapacitors may be an effective approach to meet the demand of larger electronics and thus widen their practical applications.

4 | SUMMARY AND PERSPECTIVE

In this review, the recent advances of wearable TTEG systems are systematically summarized, including their working modes and textile structure, selection of materials, energy storage and power management, and their integration into textiles. In terms of textile structures, woven textiles are suggested to be utilized in parallel contact-surfaces or symmetrical contact-surfaces due to their simple, relatively smooth with a large top surface area, stable structure, and good durability, which is suitable for CS, LS, and FT mode TTEGs. Knitted textiles are suggested to be utilized in asymmetric and easily changeable contact-surfaces due to its merits in good elasticity and ease of deformation, which is suitable for SE and CS mode TTEGs. A combination of TENGs and textiles have shown a huge platform of wearable and green power sources by harvesting energy from human motion. Through continuous research on wearable TTEG systems and related technologies, we believe that such power systems will have a drastic impact and could be applied for practical application soon.

FIGURE 2 Energy storage and the related circuit management for wearable TTEGs and their hybrid generators. A, Illustration of wearable and green power sources (the wearable energy harvester, reproduced with permission: Copyright 2017, ACS Nano.[34]). B-D, Small-size, rigid and commercial rectifier, and energy storage. B, Illustrated hybrid power textile to charge a commercial capacitor. Reproduced with permission: Copyright 2020, Springer Nature.[32] C, Self-powered disinfection system with the integration of the capacitor. Reproduced with permission: Copyright 2020, Elsevier.[35] D, Demonstration of continuously driving a smartwatch by hand tapping on the 3D orthogonal woven triboelectric nanogenerator with a power management circuit. Reproduced with permission: Copyright 2017, John Wiley and Sons.[36] E,F, Soft and wearable energy storage. E, All-textile flexible supercapacitor. Reproduced with permission: Copyright 2020, Elsevier.[170] F, Structures of TiN nanowire-based fiber supercapacitors, and integrated energy textiles. Reproduced with permission: Copyright 2016, American Chemical Society.[171] G, A woven fabric made with solid-state SC yarns. Reproduced with permission: Copyright 2015, Mascmillan.[172] H-M, All-in-one power sources. H, Structural design of the power textile that integrates a triboelectric nanogenerator and fiber-based supercapacitors. Reproduced with permission: Copyright 2017, American Chemical Society.[46] I, Schematic diagram, photograph, and charge/discharge curves of an all-textile power system that integrates a textile TEG and fiber supercapacitors. Reproduced with permission: Copyright 2020, John Wiley and Sons.[188] J, Schematic diagram and a photograph of a free-standing mode fabric triboelectric nanogenerator and woven supercapacitors. Reproduced with permission: Copyright 2020, Elsevier.[189] K, The integrated power-textile. Reproduced with permission: Copyright 2020, John Wiley and Sons.[33] L, Wearable self-charged system that integrates a single-electrode mode TEG and an electrochemical micro-supercapacitor, and the charge curves. Reproduced with permission: Copyright 2020, Elsevier.[175] M, Schematic of a fiber-based power textile, which is made of an F-TENG, an F-DSSC as an energy-harvesting fabric, and an F-SC as an energy-storing fabric. Reproduced with permission: Copyright 2016, American Association for the Advancement of Science[184]

Even though significant progress has been made, more works on fundamental issues on the high efficiency of TTEGs, energy storage and power management, and their integration are still required. And the following aspects should be carried out for a green and practical power supplying harvested energy from human motion.

1. Higher efficiency of energy harvesters is the most essential issue. The efficiency of the current TTEGs is still low. Apart from a reasonable selection of triboelectric materials, the structural design of the TTEG is especially important. How to make an efficient conversion structure that converts low frequency and irregular mechanical input of human motion into high-frequency effective contact-separation of the TTEG, which will be a breakthrough to high efficient energy harvesters. Up to now, most of the functional fibers in TTEGs are fixed inside the textiles without a relative movement or effective triboelectric contact. Textiles have multiple structural-hierarchy from fibers to fabrics. Therefore, more triboelectric fibers on the top surface should be better so that more effective contact area can be achieved. As well as these fibers are desirable to have vibrations after contact, inducing more charge transfer.
2. Enhancement of energy storage is required in terms of energy density, leakage current, lifetime, and fabrications. When using TTEGs or their hybrid generators to charge the storage devices, it often takes a relatively long time to finish the charging process. In this situation, the leakage current must be ultrasmall small so that it can be neglected during the long charging process. Yet, the leakage current is rarely discussed in the current research of wearable supercapacitors or lithium batteries. Moreover, although current supercapacitors have been made by using fiber-shapes and integrated into textile structures, it still has a long way to be a wearable power-textile due to the large size of the fiber, high rigidity, ease of damage, and high-cost.
3. The efficiency of power management should be enhanced. Although a universal power management strategy has been developed and a satisfying efficiency (~80%) can be achieved at a certain condition, the real efficiency is still low for the whole range output of the TTEGs due to the low frequency and irregular mechanical input from human motion. Moreover, the selection of the appropriate supercapacitors/batteries is also important so that their impedances and capacities can match the pulsed output of TEGs. Moreover, the power management devices are highly desirable to be embedded in textile. And thus, smaller, softer, more powerful, and even fiber-shaped power management devices are necessary in future.
4. Developing textile-based harvester systems with high security, lightweight, superior flexibility and wearability, washability, and comfort is a meaningful and promising research direction for next-generation, wearable, and green power sources. With the development of power textile, the safety issue has been increasingly concerned, especially for their application in daily use.[10] The safety concern of power textiles mainly lies in the following aspects, including electrical components of rigid nanomaterials that require a comprehensive assessment of their effect on the human body and environment, leakage of electrolyte, and overhear due to the ohmic heating. Meanwhile, functional fibers embedded into textiles could effectively avoid large deformation and damage if the textile structures were reasonable. However, if the textile structure was unreasonable, the embedded function fibers might be ease of stress-concentration which leads to the functional fibers are broken.
5. Accepting output power, there is still a huge gap between research and practical commercial applications. Herein, the working stability, various wearability, industrial fabrication, evaluation standard, and target market of the smart and power textiles should be developed or furtherly analyzed.[1] Large-scale industrial production of TTEGs is one of the basic promises for wide commercial applications. However, the functional fibers utilized for triboelectric units or supercapacitors are still too large, rigid, and/or ease of damage to produce textiles by using commercial machines. Moreover, the current TTEG systems are normally including rigid electronics. The connection between these rigid electronics and soft functional fibers are easily broken, which also bring huge challenges in washability, robustness, and conformability.

ACKNOWLEDGMENTS

The authors acknowledge financial support from the Research Grants Council, Hong Kong (Project no. 525113, 15215214, 15211016, 15200917), Hong Kong Polytechnic University, Hong Kong (Project no. 1-BBA3), and Innovation and Technology Commission, Hong Kong SAR Government (Project no. ITP/039/16TP).

CONFLICT OF INTEREST

The authors declare no conflicts of interest.

ORCID

Xiaoming Tao https://orcid.org/0000-0002-2406-0695

REFERENCES

1. Dong K, Peng X, Wang ZL. Fiber/fabric-based piezoelectric and triboelectric nanogenerators for flexible/stretchable and

wearable electronics and artificial intelligence. *Adv Mater*. 2020;32(5):1902549.

2. Tao XM. Study of fiber-based wearable energy systems. *Acc Chem Res*. 2019;52(2):307-315.
3. Kim J, Lee JH, Lee J, Yamauchi Y, Choi CH, Kim JH. Research update: hybrid energy devices combining nanogenerators and energy storage systems for self-charging capability. *Appl Mater*. 2017;5(7):073804.
4. Proto A, Penhaker M, Conforto S, Schmid M. Nanogenerators for human body energy harvesting. *Trends Biotechnol*. 2017;35(7):610-624.
5. Pu X, Hu WG, Wang ZL. Toward wearable self-charging power systems: the integration of energy-harvesting and storage devices. *Small*. 2018;14(1):1702817.
6. Hu YF, Zheng ZJ. Progress in textile-based triboelectric nanogenerators for smart fabrics. *Nano Energy*. 2019;56:16-24.
7. Luo JJ, Wang ZL. Recent advances in triboelectric nanogenerator based self-charging power systems. *Energy Storage Mater*. 2019;23:617-628.
8. Paosangthong W, Torah R, Beeby S. Recent progress on textile-based triboelectric nanogenerators. *Nano Energy*. 2019;55:401-423.
9. Huang L, Lin SZ, Xu ZS, et al. Fiber-based energy conversion devices for human-body energy harvesting. *Adv Mater*. 2020;32(5):1902034.
10. Shi JD, Liu S, Zhang LS, et al. Smart textile-integrated microelectronic systems for wearable applications. *Adv Mater*. 2020;32(5):1901958.
11. Zhang N, Chen J, Huang Y, et al. A wearable all-solid photovoltaic textile. *Adv Mater*. 2016;28(2):263-269.
12. Zhang N, Huang F, Zhao S, et al. Photo-rechargeable fabrics as sustainable and robust power sources for wearable bioelectronics. *Matter*. 2020;2(5):1260-1269.
13. Zeng W, Tao XM, Lin SP, et al. Defect-engineered reduced graphene oxide sheets with high electric conductivity and controlled thermal conductivity for soft and flexible wearable thermoelectric generators. *Nano Energy*. 2018;54:163-174.
14. Zhang LS, Lin SP, Hua T, Huang BL, Liu SR, Tao XM. Fiber-based thermoelectric generators: materials, device structures, fabrication, characterization, and applications. *Adv Energy Mater*. 2018;8(5):1700524.
15. Zhang LS, Yang B, Lin S-P, Hua T, Tao X-M. Predicting performance of fiber thermoelectric generator arrays in wearable electronic applications. *Nano Energy*. 2020;76:105117.
16. Wu C, Wang AC, Ding W, Guo H, Wang ZL. Triboelectric nanogenerator: a foundation of the energy for the new era. *Adv Energy Mater*. 2019;9(1):1802906.
17. McArdle WD, Katch FI, Katch VL. *Exercise Physiology: Energy, Nutrition, and Human Performance*. Philadelphia, PA: Lippincott Williams & Wilkins; 2010:162-177.
18. Winter DA. *Biomechanics and Motor Control of Human Movement*. Hoboken, NJ: John Wiley & Sons; 2009:82-106.
19. Riemer R, Shapiro A. Biomechanical energy harvesting from human motion: theory, state of the art, design guidelines, and future directions. *J Neuroeng Rehabil*. 2011;8(1):22.
20. Shorten MR. The energetics of running and running shoes. *J Biomech*. 1993;26:41-51.
21. Kobayashi Y, Sudo M, Miwa H, et al. Estimation accuracy of average walking speed by acceleration signals: comparison among three different sensor locations. *Proceedings of the 20th Congress of the International Ergonomics Association (IEA 2018), Vol I: Healthcare Ergonomics*. Vol 818. Switzerland: Springer; 2019:346-351.
22. Hof AL, Elzinga H, Grimmius W, Halbertsma JPK. Speed dependence of averaged EMG profiles in walking. *Gait Posture*. 2002;16(1):78-86.
23. Everyday motion. https://www.bbc.co.uk/bitesize/guides/zq4mfcw/revision/1. Accessed July 15, 2020.
24. Kaddar B, Aoustin Y, Chevallereau C. Arm swing effects on walking bipedal gaits composed of impact, single and double support phases. *Robot Auton Syst*. 2015;66:104-115.
25. Doke J, Donelan JM, Kuo AD. Mechanics and energetics of swinging the human leg. *J Exp Biol*. 2005;208(3):439-445.
26. Fan FR, Tian ZQ, Wang ZL. Flexible triboelectric generator. *Nano Energy*. 2012;1(2):328-334.
27. Wang ZL, Lin L, Chen J, Niu S, Zi Y. *Triboelectric Nanogenerators*. Switzerland: Springer; 2016:23-154.
28. Wang ZL. Triboelectric nanogenerators as new energy technology for self-powered systems and as active mechanical and chemical sensors. *ACS Nano*. 2013;7(11):9533-9557.
29. Wang ZL, Chen J, Lin L. Progress in triboelectric nanogenerators as a new energy technology and self-powered sensors. *Energ Environ Sci*. 2015;8(8):2250-2282.
30. Xie LJ, Chen XP, Wen Z, et al. Spiral steel wire based fiber-shaped stretchable and tailorable triboelectric nanogenerator for wearable power source and active gesture sensor. *Nano-Micro Lett*. 2019;11(1):39.
31. Dong K, Deng J, Ding W, et al. Versatile core-sheath yarn for sustainable biomechanical energy harvesting and real-time human-interactive sensing. *Adv Energy Mater*. 2018;8(23):1801114.
32. Chen J, Huang Y, Zhang NN, et al. Micro-cable structured textile for simultaneously harvesting solar and mechanical energy. *Nat Energy*. 2016;1(10):1-8.
33. Pu X, Song WX, Liu MM, et al. Wearable power-textiles by integrating fabric triboelectric nanogenerators and fiber-shaped dye-sensitized solar cells. *Adv Energy Mater*. 2016;6(20):1601048.
34. Yu AF, Pu X, Wen RM, et al. Core-shell-yarn-based triboelectric nanogenerator textiles as power cloths. *ACS Nano*. 2017;11(12):12764-12771.
35. Chiu CM, Ke YY, Chou TM, et al. Self-powered active antibacterial clothing through hybrid effects of nanowire-enhanced electric field electroporation and controllable hydrogen peroxide generation. *Nano Energy*. 2018;53:1-10.
36. Dong K, Deng J, Zi Y, et al. 3D orthogonal woven triboelectric nanogenerator for effective biomechanical energy harvesting and as self-powered active motion sensors. *Adv Mater*. 2017;29(38):1702648.
37. Chen CY, Chen LJ, Wu ZY, et al. 3D double-faced interlock fabric triboelectric nanogenerator for bio-motion energy harvesting and as self-powered stretching and 3D tactile sensors. *Mater Today*. 2020;32:84-93.
38. Gong J, Xu B, Yang Y, Wu M, Yang B. An adhesive surface enables high-performance mechanical energy harvesting with unique frequency-insensitive and pressure-enhanced output characteristics. *Adv Mater*. 2020;32(14):1907948.
39. Zhu G, Zhou YS, Bai P, et al. A shape-adaptive thin-film-based approach for 50% high-efficiency energy generation

through micro-grating sliding electrification. *Adv Mater*. 2014; 26(23):3788-3796.
40. Xie Y, Wang S, Niu S, et al. Grating-structured freestanding triboelectric-layer nanogenerator for harvesting mechanical energy at 85% total conversion efficiency. *Adv Mater*. 2014;26 (38):6599-6607.
41. Yang T, Zhou W, Ma P. Manufacture and property of warp-knitted fabrics with polylactic acid multifilament. *Polymers*. 2019;11(1):65.
42. Zhi C, Du M, Sun Z, et al. Warp-knitted spacer fabric reinforced syntactic foam: a compression modulus meso-mechanics theoretical model and experimental verification. *Polymers*. 2020;12(2):286.
43. Gereke T, Cherif C. A review of numerical models for 3D woven composite reinforcements. *Compos Struct*. 2019;209:60-66.
44. Bogdanovich A. An overview of three-dimensional braiding technologies. *Advances in Braiding Technology*. Cambridge, UK: Woodhead Publishing; 2016:3-78.
45. Lai YC, Deng J, Zhang SL, Niu S, Guo H, Wang ZL. Single-thread-based wearable and highly stretchable triboelectric nanogenerators and their applications in cloth-based self-powered human-interactive and biomedical sensing. *Adv Funct Mater*. 2017;27(1):1604462.
46. Dong K, Wang YC, Deng JN, et al. A highly stretchable and washable all-yarn-based self-charging knitting power textile composed of Fiber triboelectric nanogenerators and supercapacitors. *ACS Nano*. 2017;11(9):9490-9499.
47. Gong J, Xu B, Guan X, Chen Y, Li S, Feng J. Towards truly wearable energy harvesters with full structural integrity of fiber materials. *Nano Energy*. 2019;58:365-374.
48. Yang Y, Xie L, Wen Z, et al. Coaxial triboelectric nanogenerator and supercapacitor fiber-based self-charging power fabric. *ACS Appl Mater Interfaces*. 2018;10(49):42356-42362.
49. Yang Y, Sun N, Wen Z, et al. Liquid-metal-based super-stretchable and structure-designable triboelectric nanogenerator for wearable electronics. *ACS Nano*. 2018;12(2): 2027-2034.
50. Liu M, Cong Z, Pu X, et al. High-energy asymmetric supercapacitor yarns for self-charging power textiles. *Adv Funct Mater*. 2019;29(41):1806298.
51. Chandrasekhar A, Alluri NR, Saravanakumar B, Selvarajan S, Kim SJ. Human interactive triboelectric nanogenerator as a self-powered smart seat. *ACS Appl Mater Interfaces*. 2016;8 (15):9692-9699.
52. Peng X, Dong K, Ye CY, et al. A breathable, biodegradable, antibacterial, and self-powered electronic skin based on all-nanofiber triboelectric nanogenerators. *Sci Adv*. 2020;6(26): eaba9624.
53. Chu H, Jang H, Lee Y, Chae Y, J-HJNE A. Conformal, graphene-based triboelectric nanogenerator for self-powered wearable electronics. *Nano Energy*. 2016;27:298-305.
54. Su M, Brugger J, Kim BJIJOPE, Technology M-G. Simply structured wearable triboelectric nanogenerator based on a hybrid composition of carbon nanotubes and polymer layer. *Int J Precis Eng Manuf Green Technol*. 2020;7(3):683-698.
55. Chen SW, Cao X, Wang N, et al. An ultrathin flexible single-electrode triboelectric-nanogenerator for mechanical energy harvesting and instantaneous force sensing. *Adv Energy Mater*. 2017;7(1):1601255.
56. Guo H, Yeh M-H, Lai Y-C, et al. All-in-one shape-adaptive self-charging power package for wearable electronics. *ACS Nano*. 2016;10(11):10580-10588.
57. Yang Y, Zhang H, Lin Z-H, et al. Human skin based triboelectric nanogenerators for harvesting biomechanical energy and as self-powered active tactile sensor system. *ACS Nano*. 2013;7 (10):9213-9222.
58. Yang PK, Lin L, Yi F, et al. A flexible, stretchable and shape-adaptive approach for versatile energy conversion and self-powered biomedical monitoring. *Adv Mater*. 2015;27(25): 3817-3824.
59. Qi JB, Wang AC, Yang WF, et al. Hydrogel-based hierarchically wrinkled stretchable nanofibrous membrane for high performance wearable triboelectric nanogenerator. *Nano Energy*. 2020;67:104206.
60. Li S, Zhong Q, Zhong J, et al. Cloth-based power shirt for wearable energy harvesting and clothes ornamentation. *ACS Appl Mater Interfaces*. 2015;7(27):14912-14916.
61. Jung S, Lee J, Hyeon T, Lee M, Kim DHJAM. Fabric-based integrated energy devices for wearable activity monitors. *Adv Mater*. 2014;26(36):6329-6334.
62. Tong Y, Feng Z, Kim J, Robertson JL, Jia X, Johnson BN. 3D printed stretchable triboelectric nanogenerator fibers and devices. *Nano Energy*. 2020;75:104973.
63. Cheng Y, Lu X, Chan KH, et al. A stretchable fiber nanogenerator for versatile mechanical energy harvesting and self-powered full-range personal healthcare monitoring. *Nano Energy*. 2017;41:511-518.
64. Gong W, Hou C, Guo Y, et al. A wearable, fibroid, self-powered active kinematic sensor based on stretchable sheath-core structural triboelectric fibers. *Nano Energy*. 2017;39:673-683.
65. He X, Zi Y, Guo H, et al. A highly stretchable fiber-based triboelectric nanogenerator for self-powered wearable electronics. *Adv Funct Mater*. 2017;27(4):1604378.
66. Zhong J, Zhang Y, Zhong Q, et al. Fiber-based generator for wearable electronics and mobile medication. *ACS Nano*. 2014; 8(6):6273-6280.
67. Wang W, Yu AF, Liu X, et al. Large-scale fabrication of robust textile triboelectric nanogenerators. *Nano Energy*. 2020;71: 104605.
68. Zhao T, Li J, Zeng H, et al. Self-powered wearable sensing-textiles for real-time detecting environmental atmosphere and body motion based on surface-triboelectric coupling effect. *Nanotechnology*. 2018;29(40):405504.
69. Somkuwar VU, Pragya A, BJJoMS K. Structurally engineered textile-based triboelectric nanogenerator for energy harvesting application. *J Mater Sci*. 2020;55(12):5177-5189.
70. Pu X, Li LX, Song HQ, et al. A self-charging power unit by integration of a textile triboelectric nanogenerator and a flexible lithium-ion battery for wearable electronics. *Adv Mater*. 2015;27(15):2472-2478.
71. Kong TH, Lee SS, Choi GJ, Park IK. Churros-like polyvinylidene fluoride nanofibers for enhancing output performance of triboelectric nanogenerators. *ACS Appl Mater Interfaces*. 2020;12(15):17836-17844.
72. Liu HY, Wang H, Lyu Y, He CF, Liu ZH. A novel triboelectric nanogenerator based on carbon fiber reinforced composite lamina and as a self-powered displacement sensor. *Microelectron Eng*. 2020;224:111231.

73. Guo Y, Li K, Hou C, Li Y, Zhang Q, Wang H. Fluoroalkylsilane-modified textile-based personal energy management device for multifunctional wearable applications. *ACS Appl Mater Interfaces*. 2016;8(7):4676-4683.
74. Ji SH, Lee W, Yun JS. All-in-one piezo-triboelectric energy harvester module based on piezoceramic nanofibers for wearable devices. *ACS Appl Mater Interfaces*. 2020;12(16):18609-18616.
75. Zhang JH, Li Y, Hao XH. A high-performance triboelectric nanogenerator with improved output stability by construction of biomimetic superhydrophobic nanoporous fibers. *Nanotechnology*. 2020;31(21):215401.
76. Lee S, Ko W, Oh Y, et al. Triboelectric energy harvester based on wearable textile platforms employing various surface morphologies. *Nano Energy*. 2015;12:410-418.
77. Huang LB, Xu W, Tian W, et al. Ultrasonic-assisted ultrafast fabrication of polymer nanowires for high performance triboelectric nanogenerators. *Nano Energy*. 2020;71:104593.
78. Yang W, Chen J, Zhu G, et al. Harvesting energy from the natural vibration of human walking. *ACS Nano*. 2013;7(12):11317-11324.
79. Hou TC, Yang Y, Zhang H, Chen J, Chen LJ, Wang ZL. Triboelectric nanogenerator built inside shoe insole for harvesting walking energy. *Nano Energy*. 2013;2(5):856-862.
80. Kang XF, Pan CX, Chen YH, Pu X. Boosting performances of triboelectric nanogenerators by optimizing dielectric properties and thickness of electrification layer. *RSC Adv*. 2020;10(30):17752-17759.
81. Niu S, Wang X, Yi F, Zhou YS, Wang ZL. A universal self-charging system driven by random biomechanical energy for sustainable operation of mobile electronics. *Nat Commun*. 2015;6(1):1-8.
82. Kang Y, Wang B, Dai S, Liu G, Pu Y, Hu C. Folded elastic strip-based triboelectric nanogenerator for harvesting human motion energy for multiple applications. *ACS Appl Mater Interfaces*. 2015;7(36):20469-20476.
83. Bai P, Zhu G, Lin ZH, et al. Integrated multilayered triboelectric nanogenerator for harvesting biomechanical energy from human motions. *ACS Nano*. 2013;7(4):3713-3719.
84. Cong ZF, Guo WB, Guo ZH, et al. Stretchable coplanar self-charging power textile with resist-dyeing triboelectric nanogenerators and microsupercapacitors. *ACS Nano*. 2020;14(5):5590-5599.
85. Zhou T, Zhang C, Han CB, Fan FR, Tang W, Wang ZL. Woven structured triboelectric nanogenerator for wearable devices. *ACS Appl Mater Interfaces*. 2014;6(16):14695-14701.
86. Gong R, Ozgen B, Soleimani M. Modeling of yarn cross-section in plain woven fabric. *Text Res J*. 2009;79(11):1014-1020.
87. Lin CM, Lou CW, Lin JH. Manufacturing and properties of fire-retardant and thermal insulation nonwoven fabrics with FR-polyester hollow fibers. *Text Res J*. 2009;79(11):993-1000.
88. Bilisik K. Three-dimensional braiding for composites: a review. *Text Res J*. 2013;83(13):1414-1436.
89. Choi MS, Ashdown SP. Effect of changes in knit structure and density on the mechanical and hand properties of weft-knitted fabrics for outerwear. *Text Res J*. 2000;70(12):1033-1045.
90. Hays DA. Contact electrification between mercury and polyethylene: effect of surface oxidation. *J Chem Phys*. 1974;61(4):1455-1462.
91. Lowell J. Contact electrification of metals. *J Phys D*. 1975;8(1):53-63.
92. Liu CY, Bard AJ. Electrons on dielectrics and contact electrification. *Chem Phys Lett*. 2009;480(4–6):145-156.
93. Lacks DJ, Sankaran RM. Contact electrification of insulating materials. *J Phys D*. 2011;44(45):453001.
94. Mizes H, Conwell E, Salamida D. Direct observation of ion transfer in contact charging between a metal and a polymer. *Appl Phys Lett*. 1990;56(16):1597-1599.
95. Wiles JA, Fialkowski M, Radowski MR, Whitesides GM, Grzybowski BA. Effects of surface modification and moisture on the rates of charge transfer between metals and organic materials. *J Phys Chem B*. 2004;108(52):20296-20302.
96. Baytekin H, Patashinski A, Branicki M, Baytekin B, Soh S, Grzybowski BA. The mosaic of surface charge in contact electrification. *Science*. 2011;333(6040):308-312.
97. Wang S, Zi Y, Zhou YS, et al. Molecular surface functionalization to enhance the power output of triboelectric nanogenerators. *J Mater Chem A*. 2016;4(10):3728-3734.
98. Xu C, Wang AC, Zou H, et al. Raising the working temperature of a triboelectric nanogenerator by quenching down electron thermionic emission in contact-electrification. *Adv Mater*. 2018;30(38):1803968.
99. Xu C, Zhang B, Wang AC, et al. Contact-electrification between two identical materials: curvature effect. *ACS Nano*. 2019;13(2):2034-2041.
100. Xu C, Zi Y, Wang AC, et al. On the electron-transfer mechanism in the contact-electrification effect. *Adv Mater*. 2018;30(15):1706790.
101. Niu S, Liu Y, Wang S, et al. Theoretical investigation and structural optimization of single-electrode triboelectric nanogenerators. *Adv Funct Mater*. 2014;24(22):3332-3340.
102. Niu S, Liu Y, Wang S, et al. Theory of sliding-mode triboelectric nanogenerators. *Adv Mater*. 2013;25(43):6184-6193.
103. Niu S, Wang S, Lin L, et al. Theoretical study of contact-mode triboelectric nanogenerators as an effective power source. *Energ Environ Sci*. 2013;6(12):3576-3583.
104. Niu S, Liu Y, Zhou YS, Wang S, Lin L, Wang ZL. Optimization of triboelectric nanogenerator charging systems for efficient energy harvesting and storage. *IEEE Trans Electron Dev*. 2014;62(2):641-647.
105. Yang B, Zeng W, Peng ZH, Liu SR, Chen K, Tao XM. A fully verified theoretical analysis of contact-mode triboelectric nanogenerators as a wearable power source. *Adv Energy Mater*. 2016;6(16):1600505.
106. Yang B, Tao XM, Peng ZH. Upper limits for output performance of contact-mode triboelectric nanogenerator systems. *Nano Energy*. 2019;57:66-73.
107. Niu S, Liu Y, Chen X, et al. Theory of freestanding triboelectric-layer-based nanogenerators. *Nano Energy*. 2015;12:760-774.
108. Torah R, Lawrie-Ashton J, Li Y, Arumugam S, Sodano HA, Beeby S. Energy-harvesting materials for smart fabrics and textiles. *MRS Bull*. 2018;43(3):214-219.
109. Shao JJ, Jiang T, Wang ZL. Theoretical foundations of triboelectric nanogenerators (TENGs). *Sci China Technol Sci*. 2020;63(7):1087-1109.
110. Park CH, Park JK, Jeon HS, Chun BC. Triboelectric series and charging properties of plastics using the designed vertical-reciprocation charger. *J Electrostat*. 2008;66(11–12):578-583.

111. Liu SR, Zheng W, Yang B, Tao XM. Triboelectric charge density of porous and deformable fabrics made from polymer fibers. *Nano Energy*. 2018;53:383-390.
112. Zhang B, Lei J, Qi D, et al. Stretchable conductive fibers based on a cracking control strategy for wearable electronics. *Adv Funct Mater*. 2018;28(29):1801683.
113. Zou HY, Zhang Y, Guo LT, et al. Quantifying the triboelectric series. *Nat Commun*. 2019;10(1):1-9.
114. Zou HY, Guo LT, Xue H, et al. Quantifying and understanding the triboelectric series of inorganic non-metallic materials. *Nat Commun*. 2020;11(1):1-7.
115. Ge J, Sun L, Zhang FR, et al. A stretchable electronic fabric artificial skin with pressure-, lateral strain-, and flexion-sensitive properties. *Adv Mater*. 2016;28(4):722-728.
116. Cao Z, Wang R, He T, Xu F, Sun J. Interface-controlled conductive fibers for wearable strain sensors and stretchable conducting wires. *ACS Appl Mater Interfaces*. 2018;10(16):14087-14096.
117. Rathmell AR, Bergin SM, Hua YL, Li ZY, Wiley BJ. The growth mechanism of copper nanowires and their properties in flexible, transparent conducting films. *Adv Mater*. 2010;22 (32):3558-3563.
118. Wu B, Heidelberg A, Boland JJ. Mechanical properties of ultrahigh-strength gold nanowires. *Nat Mater*. 2005;4(7): 525-529.
119. Xu F, Zhu Y. Highly conductive and stretchable silver nanowire conductors. *Adv Mater*. 2012;24(37):5117-5122.
120. Sofiah A, Samykano M, Kadirgama K, Mohan R, Lah N. Metallic nanowires: mechanical properties – theory and experiment. *Appl Mater Today*. 2018;11:320-337.
121. Ye S, Rathmell AR, Chen Z, Stewart IE, Wiley BJ. Metal nanowire networks: the next generation of transparent conductors. *Adv Mater*. 2014;26(39):6670-6687.
122. Sannicolo T, Lagrange M, Cabos A, Celle C, Simonato JP, Bellet D. Metallic nanowire-based transparent electrodes for next generation flexible devices: a review. *Small*. 2016;12(44): 6052-6075.
123. Chen Y, Zhang B, Liu G, Zhuang X, Kang E-T. Graphene and its derivatives: switching ON and OFF. *Chem Soc Rev*. 2012;41 (13):4688-4707.
124. Wen L, Li F, Cheng HM. Carbon nanotubes and graphene for flexible electrochemical energy storage: from materials to devices. *Adv Mater*. 2016;28(22):4306-4337.
125. Du J, Pei S, Ma L, Cheng HM. 25th anniversary article: carbon nanotube-and graphene-based transparent conductive films for optoelectronic devices. *Adv Mater*. 2014;26(13):1958-1991.
126. Kou L, Huang T, Zheng B, et al. Coaxial wet-spun yarn supercapacitors for high-energy density and safe wearable electronics. *Nat Commun*. 2014;5(1):1-10.
127. Wang C, Wallace GG. Flexible electrodes and electrolytes for energy storage. *Electrochim Acta*. 2015;175:87-95.
128. Chen Y, Liu Z, Zhu D, et al. Liquid metal droplets with high elasticity, mobility and mechanical robustness. *Mater Horizons*. 2017;4(4):591-597.
129. Wang X, Guo R, Liu J. Liquid metal based soft robotics: materials, designs, and applications. *Adv Mater Technol*. 2019;4(2): 1800549.
130. Yu Y, Guo J, Ma B, Zhang D, Zhao Y. Liquid metal-integrated ultra-elastic conductive microfibers from microfluidics for wearable electronics. *Sci Bull*. 2020;65(20):1752-1759.
131. Bo G, Ren L, Xu X, Du Y, Dou S. Recent progress on liquid metals and their applications. *Adv Phys: X*. 2018;3(1):1446359.
132. Liu S, Sweatman K, McDonald S, Nogita K. Ga-based alloys in microelectronic interconnects: a review. *Materials*. 2018;11(8): 1384.
133. Mirabedini A, Foroughi J, Farajikhah S, Wallace GG. Correction: developments in conducting polymer fibres: from established spinning methods toward advanced applications. *RSC Adv*. 2016;6(110):108152-108152.
134. Zhao S, Li J, Cao D, et al. Recent advancements in flexible and stretchable electrodes for electromechanical sensors: strategies, materials, and features. *ACS Appl Mater Interfaces*. 2017;9(14):12147-12164.
135. Sun J, Huang Y, Fu C, et al. High-performance stretchable yarn supercapacitor based on PPy@ CNTs@ urethane elastic fiber core spun yarn. *Nano Energy*. 2016;27:230-237.
136. Liu Z, Parvez K, Li R, Dong R, Feng X, Müllen K. Transparent conductive electrodes from graphene/PEDOT: PSS hybrid inks for ultrathin organic photodetectors. *Adv Mater*. 2015;27 (4):669-675.
137. Eom J, Heo J-S, Kim M, Lee JH, Park SK, Kim Y-H. Highly sensitive textile-based strain sensors using poly (3, 4-ethylenedioxythiophene): polystyrene sulfonate/silver nanowire-coated nylon threads with poly-L-lysine surface modification. *RSC Adv*. 2017;7(84):53373-53378.
138. Fan X, Wang N, Yan F, Wang J, Song W, Ge Z. A transfer-printed, stretchable, and reliable strain sensor using PEDOT: PSS/ag NW hybrid films embedded into elastomers. *Adv Mater Technol*. 2018;3(6):1800030.
139. Fan X, Nie W, Tsai H, et al. PEDOT: PSS for flexible and stretchable electronics: modifications, strategies, and applications. *Adv Sci*. 2019;6(19):1900813.
140. Lu Z, Foroughi J, Wang C, Long H, Wallace GG. Superelastic hybrid CNT/graphene fibers for wearable energy storage. *Adv Energy Mater*. 2018;8(8):1702047.
141. Bießmann L, Saxena N, Hohn N, Hossain MA, Veinot JG, Müller-Buschbaum P. Highly conducting, transparent PEDOT: PSS polymer electrodes from post-treatment with weak and strong acids. *Adv Electron Mater*. 2019;5(2): 1800654.
142. Jeon S-B, Park S-J, Kim W-G, et al. Self-powered wearable keyboard with fabric based triboelectric nanogenerator. *Nano Energy*. 2018;53:596-603.
143. Matweb. Overview of materials for polytetrafluoroethylene (PTFE), molded. http://www.matweb.com/search/datasheet_print.aspx?matguid=4d14eac958e5401a8fd152e1261b6843. Accessed July 14, 2020.
144. Fiber Properties | Properties of Textile Fibers | Primary Properties of Textile Fibers. https://textilelearner.blogspot.com/2012/01/fiber-properties-properties-of-textile.html. Accessed July 14, 2020.
145. PE & HDPE PE100 Pipe: Properties and Types. https://www.pe100plus.com/PE-Pipes/Technical-guidance/Trenchless/Methods/PE-Pipe-i1341.html. Accessed July 14, 2020.
146. HDPE. https://dielectricmfg.com/knowledge-base/polyethylene/. Accessed July 14, 2020.
147. Polyethylene (HDPE/LDPE). https://designerdata.nl/materials/plastics/thermo-plastics/high-density-polyetheen. Accessed July 14, 2020.

148. Overview of materials for polyimide. http://www.matweb.com/search/DataSheet.aspx?MatGUID=ab35b368ab9c40848f545c35bdf1a672&ckck=1. Accessed July 14, 2020.
149. Yu WD. *Textile Material Science*. China: China Textile & Apparel Press; 2006;396-400.
150. Periyasamy AP, Ramamoorthy SK, Rwawiire S, Zhao Y. Sustainable wastewater treatment methods for textile industry. *Sustainable Innovations in Apparel Production*. Singapore: Springer; 2018:21-87.
151. Standard Moisture Regain and Moisture Content of Fibers. https://textilecalculation.blogspot.com/2015/08/standard-moisture-regain-and-moisture.html. Accessed July 14, 2020.
152. Elongation at Break. https://omnexus.specialchem.com/polymer-properties/properties/elongation-at-break. Accessed July 14, 2020.
153. Liu HJ, Qi RL. Properties of pure chitosan fiber. *Text Auxil*. 2018;35(3):31-33.
154. Glass Fiber | Physical And Chemical Properties of Glass Fiber. http://textilefashionstudy.com/glass-fiber-physical-and-chemical-properties-of-glass-fiber/. Accessed July 14, 2020.
155. Physical and Chemical Properties of Wool Fiber. https://textilelearner.blogspot.com/2015/12/physical-and-chemical-properties-of.html. Accessed July 14, 2020.
156. Huang XX, Tao XM, Zhang ZH, Chen P. Properties and performances of fabrics made from bio-based and degradable polylactide acid/poly (hydroxybutyrate-co-hydroxyvalerate) (PLA/PHBV) filament yarns. *Text Res J*. 2017;87(20):2464-2474.
157. Cupro Fiber. http://cameo.mfa.org/wiki/Cupro_fiber. Accessed July 14, 2020.
158. Zhang S, Chen C, Duan C, et al. Regenerated cellulose by the lyocell process, a brief review of the process and properties. *BioResources*. 2018;13(2):4577-4592.
159. Chen J. Synthetic textile fibers: regenerated cellulose fibers. *Textiles and Fashion*. Cambridge, UK: Woodhead Publishing; 2015:79-95.
160. Thermoplastic Polyamide (Nylon 6). https://www.substech.com/dokuwiki/doku.php?id=thermoplastic_polyamide_nylon_6. Accessed July14, 2020.
161. Microstructures and Mechanical Properties of Silks of Silkworm and Honeybee. https://pubmed.ncbi.nlm.nih.gov/20026439/. Accessed July 14, 2020.
162. Silk Fiber || Physical and Chemical Properties of Silk. http://textilefashionstudy.com/silk-fiber-physical-and-chemical-properties-of-silk/. Accessed July 14, 2020.
163. Polyurethane. https://www.efunda.com/Materials/polymers/properties/polymer_datasheet.cfm?MajorID=PU&MinorID=1. Accessed July 14, 2020.
164. PUR (Rubber) Polyurethane Rubber. https://designerdata.nl/materials/plastics/rubbers/polyurethane-rubber. Accessed July 14, 2020.
165. Overview of Materials for Nylon 66, Unreinforced. http://www.matweb.com/search/datasheettext.aspx?matguid=a2e79a3451984d58a8a442c37a226107. Accessed July 14, 2020.
166. Properties of Nylon 6 & Nylon 6,6 Fiber | Comparison/Different between Nylon 6 & Nylon 6,6 Fiber. https://textilelearner.blogspot.com/2013/05/physical-properties-of-nylon-6-nylon-66.htmlPhysical. Accessed July 14, 2020.
167. Mazur K, Kuciel S. Mechanical and hydrothermal aging behaviour of polyhydroxybutyrate-co-valerate (PHBV) composites reinforced by natural fibres. *Molecules*. 2019;24(19):3538.
168. Farah S, Anderson DG, Langer R. Physical and mechanical properties of PLA, and their functions in widespread applications—a comprehensive review. *Adv Drug Deliv Rev*. 2016;107:367-392.
169. Avinc O, Khoddami A. Overview of poly(lactic acid) (PLA) fibre: part I: production, properties, performance, environmental impact, and end-use applications of poly(lactic acid) fibres. *Fibre Chem*. 2009;41:391-401.
170. Laforgue A. All-textile flexible supercapacitors using electrospun poly (3, 4-ethylenedioxythiophene) nanofibers. *J Power Sources*. 2011;196(1):559-564.
171. Chai Z, Zhang N, Sun P, et al. Tailorable and wearable textile devices for solar energy harvesting and simultaneous storage. *ACS Nano*. 2016;10(10):9201-9207.
172. Liu L, Yu Y, Yan C, Li K, Zheng Z. Wearable energy-dense and power-dense supercapacitor yarns enabled by scalable graphene-metallic textile composite electrodes. *Nat Commun*. 2015;6(1):1-9.
173. Wang J, Li X, Zi Y, et al. A flexible fiber-based supercapacitor–triboelectric-nanogenerator power system for wearable electronics. *Adv Mater*. 2015;27(33):4830-4836.
174. Song Y, Zhang JX, Guo H, et al. All-fabric-based wearable self-charging power cloth. *Appl Phys Lett*. 2017;111(7):73901.
175. Jiang Q, Wu C, Wang Z, et al. MXene electrochemical microsupercapacitor integrated with triboelectric nanogenerator as a wearable self-charging power unit. *Nano Energy*. 2018;45:266-272.
176. Li S, Peng W, Wang J, et al. All-elastomer-based triboelectric nanogenerator as a keyboard cover to harvest typing energy. *ACS Nano*. 2016;10(8):7973-7981.
177. Wang X, Yin Y, Yi F, et al. Bioinspired stretchable triboelectric nanogenerator as energy-harvesting skin for self-powered electronics. *Nano Energy*. 2017;39:429-436.
178. Zhou C, Yang Y, Sun N, et al. Flexible self-charging power units for portable electronics based on folded carbon paper. *Nano Res*. 2018;11(8):4313-4322.
179. Bhatia D, Lee J, Hwang HJ, Baik JM, Kim S, Choi D. Design of mechanical frequency regulator for predictable uniform power from triboelectric nanogenerators. *Adv Energy Mater*. 2018;8(15):1702667.
180. Xi F, Pang Y, Li W, et al. Universal power management strategy for triboelectric nanogenerator. *Nano Energy*. 2017;37:168-176.
181. Xiong G, Meng C, Reifenberger RG, Irazoqui PP, Fisher TS. A review of graphene-based electrochemical microsupercapacitors. *Electroanalysis*. 2014;26(1):30-51.
182. Zi Y, Guo H, Wang J, et al. An inductor-free auto-power-management design built-in triboelectric nanogenerators. *Nano Energy*. 2017;31:302-310.
183. Zi Y, Wang J, Wang S, et al. Effective energy storage from a triboelectric nanogenerator. *Nat Commun*. 2016;7(1):1-8.
184. Wen Z, Yeh M-H, Guo H, et al. Self-powered textile for wearable electronics by hybridizing fiber-shaped nanogenerators, solar cells, and supercapacitors. *Sci Adv*. 2016;2(10):e1600097.
185. Zhong X, Yang Y, Wang X, Wang ZL. Rotating-disk-based hybridized electromagnetic-triboelectric nanogenerator for scavenging biomechanical energy as a mobile power source. *Nano Energy*. 2015;13:771-780.

186. Wang X, Wang ZL, Yang Y. Hybridized nanogenerator for simultaneously scavenging mechanical and thermal energies by electromagnetic-triboelectric-thermoelectric effects. *Nano Energy*. 2016;26:164-171.
187. Yang Y, Zhang H, Lee S, Kim D, Hwang W, Wang ZL. Hybrid energy cell for degradation of methyl orange by self-powered electrocatalytic oxidation. *Nano Lett*. 2013;13(2):803-808.
188. Pu X, Li L, Liu M, et al. Wearable self-charging power textile based on flexible yarn supercapacitors and fabric nanogenerators. *Adv Mater*. 2016;28(1):98-105.
189. Chen J, Guo H, Pu X, Wang X, Xi Y, Hu C. Traditional weaving craft for one-piece self-charging power textile for wearable electronics. *Nano Energy*. 2018;50:536-543.

AUTHOR BIOGRAPHIES

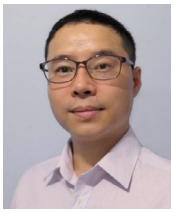

Bao Yang received his BS degree (2007) in engineering mechanics and his PhD degree (2012) in solid mechanics from the South China University of Technology, China. Since 2013, he joined the group of Prof Xiaoming Tao as a postdoc fellow/research associate/research fellow in the Research Center for Smart Wearable Technology and Institute of textiles and clothing, the Hong Kong Polytechnic University. His current research focuses on wearable electronics and photonics, energy harvesting technology, impact dynamics, and bionic materials and structures.

Xiong Ying obtained her BE degree in textile engineering in 2016 from Jiangnan University, China. She joined the group of Prof Tao Xiaoming as a research assistant in the Institute of textiles and clothing, the Hong Kong Polytechnic University, in 2016. She is currently pursuing a PhD degree in PolyU. Her research interests include wearable textile-based sensors and medical compression products.

Xiaoming Tao is Chair Professor of Textile Technology, Director of Research Centre for Smart Wearable Technology, Institute of Textiles and Clothing, The Hong Kong Polytechnic University. She obtained a BEng in textile engineering from East China Institute of Textile Science and Technology with a first class prize and a PhD in textile physics from the University of New South Wales in Australia. Prof. Tao is former World President of Textile Institute from 2007 to 2010, an elected Fellow of the Textile Institute, elected Fellow of American Society of Mechanical Engineering, and elected Fellow of the Royal Society of Arts, Manufacture, and Commercial Applications.

How to cite this article: Yang B, Xiong Y, Ma K, Liu S, Tao X. Recent advances in wearable textile-based triboelectric generator systems for energy harvesting from human motion. *EcoMat*. 2020;2: e12054. https://doi.org/10.1002/eom2.12054